Trident cold atmospheric plasma blocks three cancer survival pathways to overcome therapy resistance

Bo Guo[a,b,1], Anthony D. Pomicter[c,1], Francis Li[a], Sudhir Bhatt[a], Chen Chen[a,d], Wen Li[b], Miao Qi[d], Chen Huang[b], Michael W. Deininger[c,e], Michael G. Kong[a,f,2,3], and Hai-Lan Chen[a,2,3]

[a]Frank Reidy Center for Bioelectrics, Old Dominion University, Norfolk, VA 23508; [b]Department of Cell Biology and Genetics, School of Basic Medical Sciences, Xi'an Jiaotong University Health Science Center, Xi'an, Shaanxi 710061, People's Republic of China; [c]Huntsman Cancer Institute, University of Utah, Salt Lake City, UT 84112; [d]State Key Laboratory of Electrical Insulation and Power Equipment, Center for Plasma Biomedicine, Xi'an Jiaotong University, Xi'an, Shaanxi 710049, People's Republic of China; [e]Division of Hematology and Hematologic Malignancies, University of Utah, Salt Lake City, UT 84112; and [f]Department of Electrical and Computer Engineering, Old Dominion University, Norfolk, VA 23529

Edited by David Weitz, Division of Engineering and Applied Science, Department of Physics, Harvard University, Cambridge, MA, and approved November 1, 2021 (received for review April 16, 2021)

Therapy resistance is responsible for most cancer-related death and is mediated by the unique ability of cancer cells to leverage metabolic conditions, signaling molecules, redox status, and other pathways for their survival. Interestingly, many cancer survival pathways are susceptible to disturbances in cellular reactive oxygen species (ROS) and may therefore be disrupted by exogenous ROS. Here, we explore whether trident cold atmospheric plasma (Tri-CAP), a gas discharge with exceptionally low-level ROS, could inhibit multiple cancer survival pathways together in a murine cell line model of therapy-resistant chronic myeloid leukemia (CML). We show that Tri-CAP simultaneously disrupts three cancer survival pathways of redox deregulation, glycolysis, and proliferative AKT/mTOR/HIF-1α signaling in this cancer model. Significantly, Tri-CAP blockade induces a very high rate of apoptotic death in CML cell lines and in primary CD34$^+$ hematopoietic stem and progenitor cells from CML patients, both harboring the therapy-resistant T315I mutation. In contrast, nonmalignant controls are minimally affected by Tri-CAP, suggesting it selectively targets resistant cancer cells. We further demonstrate that Tri-CAP elicits similar lethality in human melanoma, breast cancer, and CML cells with disparate, resistant mechanisms and that it both reduces tumor formation in two mouse models and improves survival of tumor-bearing mice. For use in patients, administration of Tri-CAP may be extracorporeal for hematopoietic stem cell transplantation therapy, transdermal, or through its activated solution for infusion therapy. Collectively, our results suggest that Tri-CAP represents a potent strategy for disrupting cancer survival pathways and overcoming therapy resistance in a variety of malignancies.

therapy-resistant cancers | cancer survival pathways | cold atmospheric plasma | chronic myeloid leukemia

Targeted cancer therapies improve progression-free survival but rapidly become tolerated (1), leading to therapy resistance that is responsible for most cancer-related deaths (2, 3). As an example, chronic myeloid leukemia (CML) with the T315I mutation acquired resistance to ponatinib, the only effective drug, within 1 y of its approval by the US Food and Drug Administration (FDA) (4). Similarly, 90% of non–small cell lung cancer patients who respond to gefitinib succumb to disease progression within 2 y (5). Thus, the arms race of chasing each cancer mutation with a new inhibitor is not an efficient way to address therapy resistance. Combining several existing therapies that target multiple cancer survival pathways offers one solution to the problem; however, resistance has been already reported in clinical trials testing this strategy (6). Given these observations, we wonder whether disparate cancer targets might share a common vulnerability and if targeting this shared vulnerability with a single therapy could lead to a broadly effective strategy to overcome therapy resistance.

Cancer cells evade therapy by flexibly exploiting diverse survival pathways, including the cancer hallmarks of glycolytic metabolism for synthesis of ATP and macromolecules, deregulated cellular redox balance to resist cell death, and sustained proliferative signaling (7). Alarmingly, cross-talks between these pathways can mediate additional survival mechanisms; for example, glycolysis replenishes antioxidants to aid redox deregulation, and proliferative signaling promotes glycolysis (8). These mutually perpetuating pathways present a formidable barrier to overcoming therapy resistance. Interestingly, however, cellular reactive oxygen species (ROS) is aberrantly elevated in malignant cells and is intimately involved in the regulation of glycolysis (8, 9), redox deregulation (10), and proliferative signaling (11), suggesting its potential as a common vulnerability. We hypothesize that targeting this feature with exogenous ROS from cold atmospheric plasma (CAP), a gas discharge that electrically generates diverse ROS, photons, and transient electric field (Fig. 1 *A* and *B*), might represent an effective strategy to

Significance

In many malignancies, resistance to targeted therapy emerges rapidly and leads to disease progression and mortality. Here, we show that trident cold atmospheric plasma (Tri-CAP), a reactive oxygen species–producing gas discharge, simultaneously blocks three cancer survival pathways, including deregulated redox balance, glycolysis, and proliferative signaling, in a mouse cell line model of therapy-resistant chronic myeloid leukemia (CML). This activity leads to high-rate apoptotic death in these CML cell lines and primary CD34$^+$ hematopoietic stem and progenitor cells from CML patients, while minimally affecting nonmalignant control cells. Furthermore, Tri-CAP reduces tumor formation and prolongs the survival of tumor-bearing mice in mouse models of CML. Thus, treatment with Tri-CAP may be an effective strategy for overcoming therapy resistance in human cancers.

Author contributions: M.W.D., M.G.K., and H.-L.C. designed research; B.G., F.L., S.B., C.C., W.L., M.Q., and M.G.K. performed research; B.G., A.D.P., F.L., C.H., M.G.K., and H.-L.C. analyzed data; and B.G., A.D.P., M.G.K., and H.-L.C. wrote the paper.

Competing interest statement: M.W.D. consults for Adelphi, Ascentage Pharma, Blueprint, BMS, CTI BioPharma, Fusion Pharma, Novartis, Pfizer Sangamo, and Takeda and receives honoraria or research support from Adelphi, Ascentage Pharma, Ariad, Blueprint, BMS, Celgene, CTI BioPharma, Dispersol, Fusion Pharma, Galena, Gilead, Humana, Incyte, Medscape, Novartis, Pfizer, Sangamo, Takeda, and TRM.

This article is a PNAS Direct Submission.

[1]B.G. and A.D.P. contributed equally to this work.

[2]M.G.K. and H.-L.C. contributed equally to this work.

[3]To whom correspondence may be addressed. Email: mkong@odu.edu or h1chen@odu.edu.

This article contains supporting information online at http://www.pnas.org/lookup/suppl/doi:10.1073/pnas.2107220118/-/DCSupplemental.

Published December 16, 2021.

overcome therapy resistance. CAP has attracted significant interest because of its many applications in medicine and industry (12). In patients, CAP is approved by the FDA as a catheter-guided scalpel for routine oncology and neurology surgery (13) and has shown efficacy in clinical trials for the treatment of head and neck cancer (14). Saline pretreated by CAP, known as plasma-activated solution (PAS), is approved for use in humans in clinical trials (15). Other administration options are demonstrated in animal models, as an intraperitoneal or infusion therapy with PAS (16), or transdermally via microneedles with CAP (17).

Here, we test our hypothesis that CAP simultaneously disrupts multiple survival pathways in therapy-resistant cancer cells by exploring its ROS concentration range that spans many orders of magnitude (18). This is challenging, however, since ROS produced by cancer therapy can promote cancer cell survival pathways, including the oncogenic hypoxia-inducible factor (HIF)-1α pathway (19). As a case study, we consider CML, a primary example of malignancies defined by a unique molecular event, the BCR-ABL1 oncogene. Its T315I mutation (BCR-ABL1^{T315I}) confers resistance to all approved inhibitors, except ponatinib, which is itself limited by resistance (4) and life-threatening intolerance (20). Critically, we show that a novel CAP regime, with its hydrogen peroxide (H_2O_2) well below previously tested for treating cancer cells, blocks the above-mentioned three cancer survival pathways together in resistant BCR-ABL1^{T315I} cells (Fig. 1*C*). This trident CAP (Tri-CAP), named for its simultaneous blockade of these three pathways, induces very high-rate apoptotic death in BCR-ABL1^{T315I} cell lines and in primary CD34$^+$ hematopoietic stem and progenitor cells from CML patients with the T315I mutation, while having minimal effect on their nonmalignant control cells. In addition, Tri-CAP displays similar lethality against therapy-resistant human melanoma, breast cancer, and CML cells of disparate, resistant mechanisms, suggesting that it targets a shared vulnerability in these malignant cells. Lastly, Tri-CAP reduces tumor formation and prolongs survival of tumor-bearing mice in mouse models of CML. Given these findings, we suggest that Tri-CAP represents a potent novel cancer treatment paradigm that can be used either to complement existing therapies or as a monotherapy for overcoming therapy resistance in a variety of malignancies.

Results and Discussion

Tri-CAP Targets Therapy Resistance with Exceptionally Low-Level and Pulsed ROS. An ideal intervention for therapy resistance would simultaneously elicit selective cancer cell death and inhibit cancer cell survival pathways—a formidable challenge. For ROS-generating therapies, one dilemma is that H_2O_2 at its apoptotic concentrations may promote oncogenic HIF-1α (21). Indeed, we find that H_2O_2-induced apoptosis becomes significant after $H_2O_2 \geq 50$ μM in BCR-ABL1^{T315I} cells, but HIF-1α protein expression is already elevated by H_2O_2 as low as 10 μM (*SI Appendix*, Fig. S1), making it difficult to both kill cancer cells and block their survival pathways with this molecule alone. We hypothesize that Tri-CAP can kill cancer cells with the synergy of its diverse ROS at a very low level (e.g., below the 10-μM H_2O_2 threshold for HIF-1α activation) and that such low-level ROS has the ability to simultaneously inhibit multiple cancer survival pathways.

To test this hypothesis, we generate Tri-CAP using a plasma jet in flowing argon containing 3% oxygen at 1.9 L/min, under conditions that favor low-ROS generation, including a large 30-mm distance from the electrode to the cell medium and a low 3.8-W electrical power at 21.7 kHz (*SI Appendix*, Fig. S2 *A* and *B*). Tri-CAP minimally affects the temperature and pH of cell-free Roswell Park Memorial Institute (RPMI)-1640 medium (*SI Appendix*, Fig. S3) and is stable once established (Fig. 2*A*). Its 60-s treatment produces 1.7 μM H_2O_2 that falls to

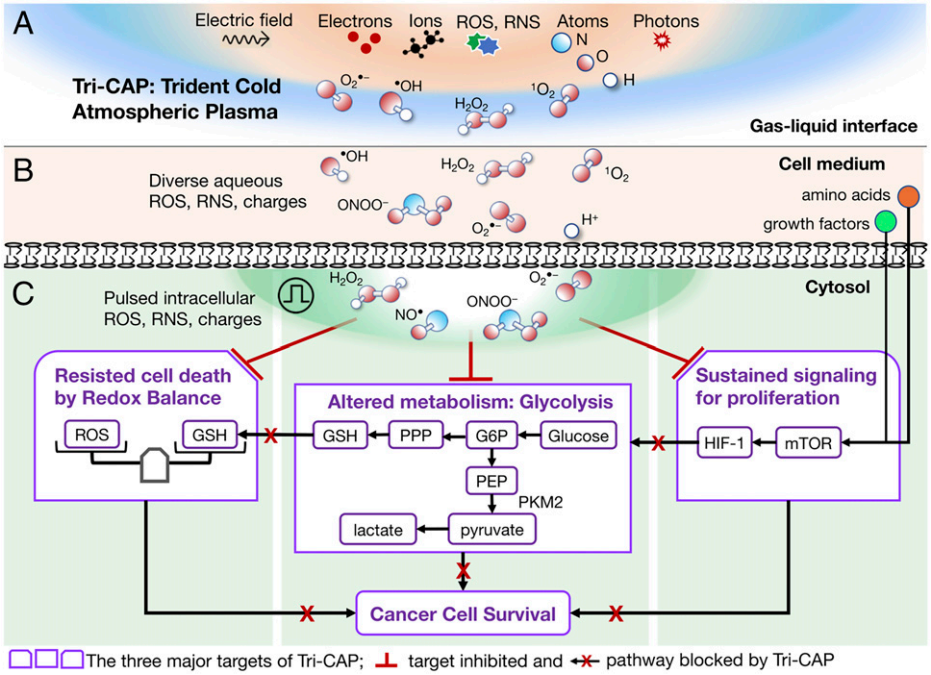

Fig. 1. Schematic overview of our hypothesis for how Tri-CAP leads to blockade of three cancer survival pathways for overcoming therapy resistance. (*A*) Tri-CAP generates exceptionally low levels of ROS, charges and atoms, photons, and transient electric fields in ambient air. (*B*) This leads to formation of diverse, low-level, aqueous ROS and charges in the cell medium. (*C*) Tri-CAP–induced pulsed elevation of diverse intracellular ROS simultaneously disrupts three key cancer survival pathways—deregulated redox balance, glycolysis, and sustained proliferative signaling—in therapy-resistant cancer cells. RNS, reactive nitrogen species; G6P, glucose-6-phosphate; PEP, phosphoenolpyruvate.

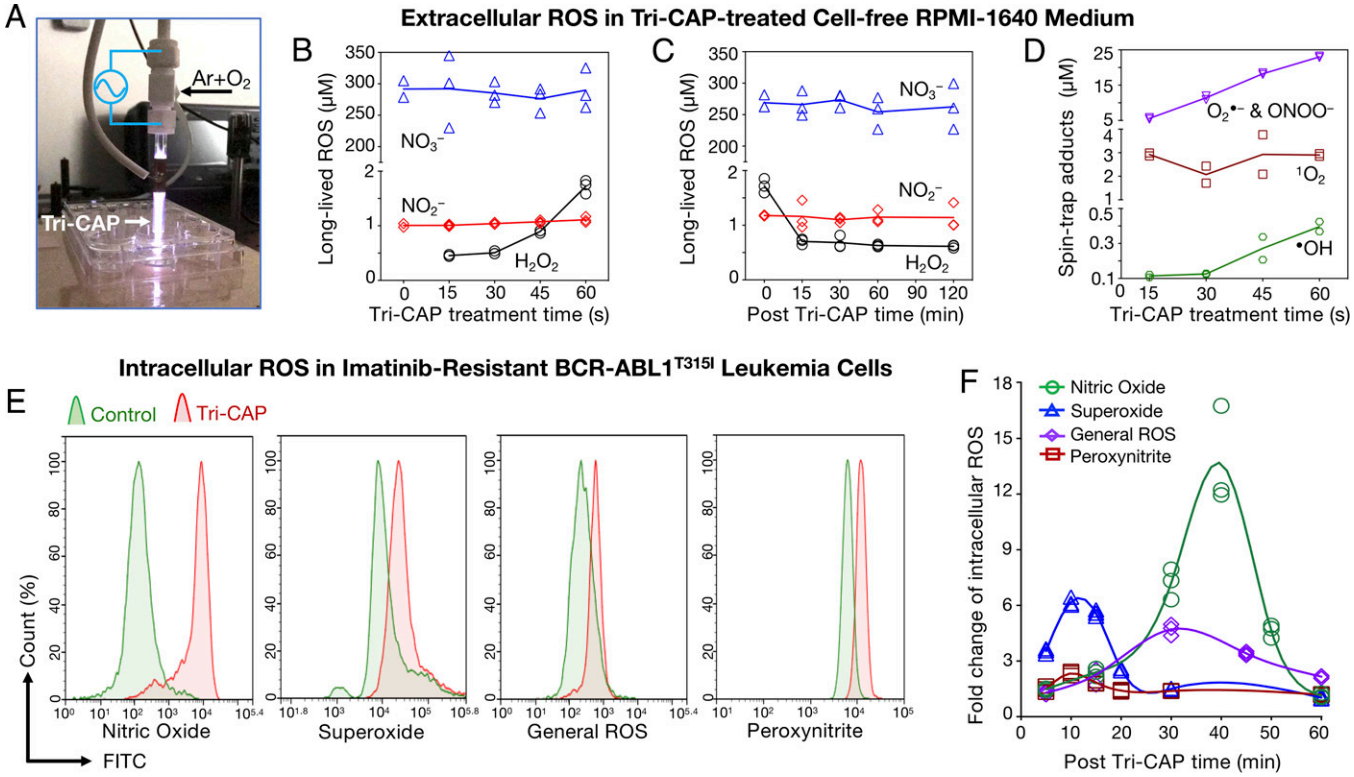

Fig. 2. Tri-CAP produces very low-level ROS in cell-free medium and transiently elevates intracellular ROS in resistant BCR-ABL1^{T315I} cell lines. (*A*) Tri-CAP in the form of a plasma jet in flowing argon with 3% O_2 that is passing through a two-electrode assembly. In cell-free RPMI-1640 medium. (*B*) A 60-s Tri-CAP treatment produces low-level H_2O_2 and induces little change in NO_2^- and NO_3^- levels. (*C*) H_2O_2 falls to 0.7 μM in 15 min, and NO_2^- and NO_3^- undergo little change post–Tri-CAP treatment. (*D*) Spin trap adduct concentrations of short-lived ROS increase with Tri-CAP treatment time (n = 3). (*E*) In imatinib-resistant BCR-ABL1^{T315I} cell lines, Tri-CAP treatment increases intracellular $^{\bullet}NO$, $O^{\bullet-}$, general ROS, and $ONOO^-$. (*F*) These increases are transient and fall toward basal levels of intracellular ROS in ~20 to 60 min (n = 3). FITC, fluorescein isothiocyanate.

0.7 μM by 15-min posttreatment (Fig. 2 *B* and *C*). This is much lower than the ~10-μM threshold of H_2O_2 for the activation of HIF-1α. It is also below H_2O_2 levels associated with the vast majority of 151 CAP regimens for cancer cell treatment (*SI Appendix*, Fig. S4 and Tables S1–S3), suggesting that Tri-CAP operates with exceptionally low-level ROS. On the other hand, nitrite (NO_2^-) and nitride (NO_3^-) from calcium nitrate in the RPMI medium are largely unchanged during and after Tri-CAP treatment (Fig. 2 *B* and *C*), unlike current plasma jets that increase NO_2^- and NO_3^- in cell medium (22).

In addition, Tri-CAP produces diverse, short-lived ROS, including singlet oxygen ($^1O_2$), superoxide ($O_2^{\bullet-}$), hydroxyl radical ($^{\bullet}OH$), nitric oxide ($^{\bullet}NO$), and peroxynitrite ($ONOO^-$), in the cell medium, detected with spin traps to form spin trap adducts and quantified with electron spin resonance (ESR) spectrometry (23), as shown in *SI Appendix*, Fig. S5 *A* and *B*. In particular, we find that Tri-CAP increases spin trap adducts of $^{\bullet}OH$, $^1O_2$, and the sum of $O_2^{\bullet-}$ and $ONOO^-$ to 0.36, 2.8, and 22.6 μM, respectively (Fig. 2*D*); $^{\bullet}NO$ is below the ESR detection limit of ~100 nM. Critically, within ~30 s post–Tri-CAP treatment, these short-lived ROS fall below the ESR detection limit (*SI Appendix*, Fig. S5*C*). These levels are distinctly low compared with many current plasma jets, which produce, for example, spin trap adducts of $^{\bullet}OH$ in the range of several tens of micromolar (24). It is worth noting that plasma jets at higher electrical power than Tri-CAP are approved to treat human tumors (13, 14).

To assess the effect of Tri-CAP treatment on cellular ROS, we use a mouse Ba/F3 cell line model of CML, including imatinib-resistant BCR-ABL1^{T315I} cells, imatinib-sensitive BCR-ABL1^{p210} cells, and normal parental cells (25). This model is commonly used to evaluate selectivity of therapeutics, as the parental cells require interleukin-3 supplementation for survival, whereas the BCR-ABL1$^+$ variants rely on signaling from this oncogene. We select one 60-s Tri-CAP treatment as it induces highly selective death of resistant BCR-ABL1^{T315I} cells, with minimal effect on parental cells (*SI Appendix*, Fig. S6). For BCR-ABL1^{T315I} cells treated with 60 s Tri-CAP, intracellular levels of their general ROS (mainly H_2O_2), $O_2^{\bullet-}$, $ONOO^-$, and $^{\bullet}NO$ peak within 10 to 45 min and then fall to near their basal levels after 20 to 60 min (Fig. 2 *E* and *F*). This pulsed, intracellular ROS elevation is much shorter in duration than the typical 24 h reported for current plasma jets (22). Collectively, these results demonstrate that Tri-CAP produces exceptionally low-level, extracellular ROS and sharp, pulsed elevation of intracellular ROS in resistant cancer cells, a largely uncharted ROS regime that leads to selective lethality in resistant cancer cells.

Two-Pronged Disruption of Redox Balance with Tri-CAP. The low-level ROS generated by Tri-CAP suggests it may disrupt critical cancer cell survival pathways, such as redox deregulation. To test this possibility, we assess both intracellular ROS and cellular antioxidant activity in all three Ba/F3 cell lines. Compared to untreated controls, intracellular ROS levels are highly elevated in both BCR-ABL1$^+$ cell lines in response to 60-s Tri-CAP treatment, whereas they are only minimally increased in parental cells (Fig. 3*A*). For example, intracellular $O_2^{\bullet-}$ increases by 5.7- to 6.8-fold in BCR-ABL1$^+$ cells and by only 1.3-fold in parental cells. Next, we evaluate antioxidant activity based on the ratio of reduced glutathione (GSH) to glutathione disulfide (GSSG). GSH is the major cellular, ROS-scavenging system for replenishing antioxidant enzymes, and GSSG is

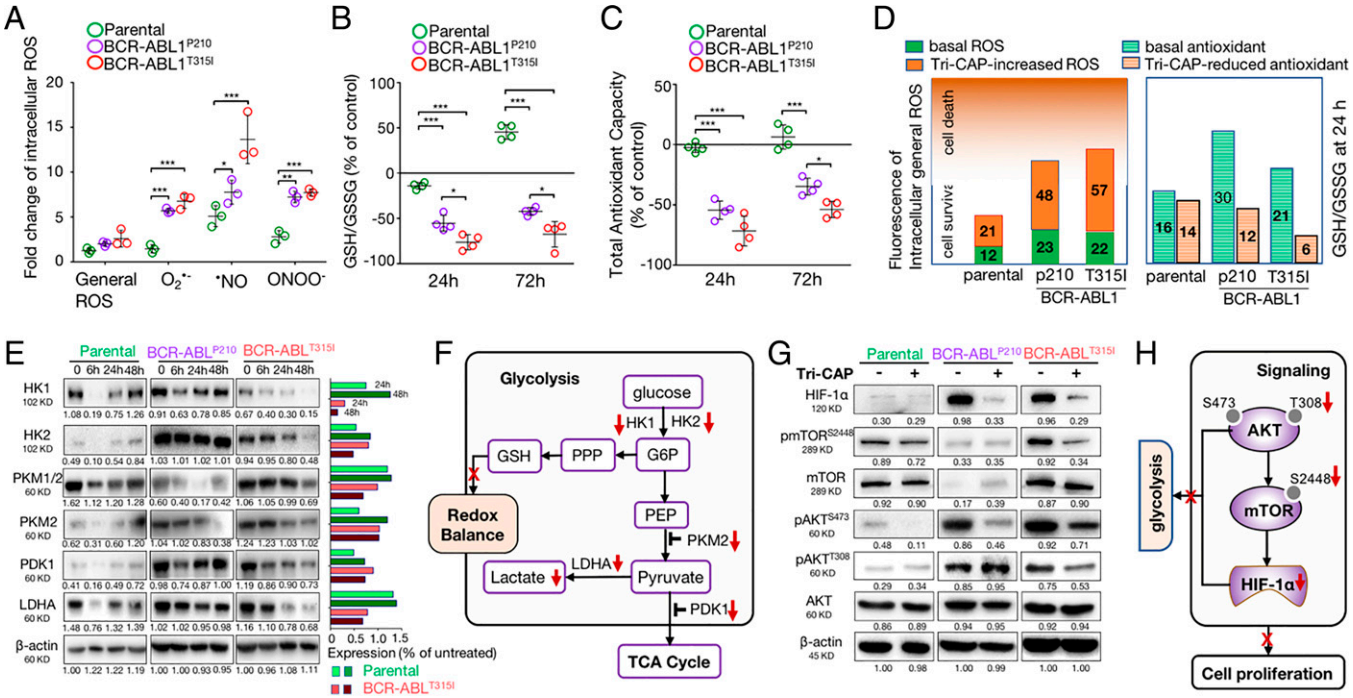

Fig. 3. Tri-CAP treatment induces a widespread blockade of cancer survival pathways, including deregulated redox balance, glycolysis, and proliferative signaling in BCR-ABL1$^+$ cells, while having little impact on parental cells. Tri-CAP treatment for 60 s induces a significant elevation of diverse intracellular ROS ($n = 3$) (*A*), sustained reduction of the GSH to GSSG ratio (*B*), and total antioxidant capacity ($n = 4$) (*C*), preferentially leading to excessive oxidative stress and reduced antioxidant defense in resistant BCR-ABL1^{T315I} cells relative to parental cells (*D*). (*E*) Tri-CAP treatment further reduces protein expression levels of six glycolytic enzymes, as evident from quantification of band intensities shown at right ($n = 3$). (*F*) These effects are predicted to disrupt glycolysis at multiple enzymatic points, thereby impeding cross-talk for supporting the maintenance of redox balance in resistant BCR-ABL1^{T315I} cells. Tri-CAP preferentially reduces protein expression of HIF-1α and blocks phosphorylation of mTOR and AKT at 6-h posttreatment in BCR-ABL1$^+$ cells ($n = 3$) (*G*), thus facilitating attenuation of the AKT/mTOR/HIF-1α signaling pathway at multiple nodes (*H*). $^*P < 0.05$, $^{**}P < 0.01$, and $^{***}P < 0.001$. TCA, tricarboxylic acid.

oxidized glutathione (9). We find that both GSH:GSSG ratio and total antioxidant capability are persistently attenuated from 24- to 72-h post–Tri-CAP treatment in BCR-ABL$^+$ cells, whereas they are elevated above their basal levels at 72 h in parental cells (Fig. 3 *B* and *C*). Notably, we observe preferential disruption of both intracellular general ROS and the GSH:GSSG ratio after Tri-CAP treatment in BCR-ABL1^{T315I} cells (Fig. 3*D*). Measurement of intracellular •NO further supports the selective impact of Tri-CAP on BCR-ABL1$^+$ cells (*SI Appendix*, Fig. S7). Together, these results indicate that Tri-CAP delivers two-pronged disruption of redox deregulation in BCR-ABL1$^+$ cell lines: excessive ROS production and attenuated antioxidant defense. In contrast, parental cells regain redox balance quickly after Tri-CAP treatment.

Tri-CAP Treatment Inhibits Multiple Key Targets in Cancer Metabolism and Reduces Lactate Production. Unlike normal cells that generally utilize the tricarboxylic acid cycle to generate energy, malignant cells often exploit anaerobic respiration to meet their energy needs (8). In this process, glucose is converted to pyruvate by glucose transporters (e.g., GLUT1) and glycolytic enzymes, producing ATP and lactate. Specifically, hexokinases (e.g., HK1 and HK2) catalyze the first step in glucose metabolism to yield glucose-6-phosphate. Then, pyruvate dehydrogenase (PDH) kinases (e.g., PDK1 and PDK3) increase the pyruvate–lactate conversion rate in the cytosol through negative regulation of PDH. Lastly, lactate dehydrogenase A (LDHA) catalyzes the pyruvate–lactate conversion (9). Critically, pyruvate kinase isozyme M2 (PKM2) reduces the rate of glucose–pyruvate flux, thereby directing glucose intermediates to the pentose phosphate pathway (PPP) for synthesis of macromolecules and reduced nicotinamide adenine dinucleotide phosphate (NADPH), which replenishes GSH (9) (*SI Appendix*, Fig. S8). Lactate exported to the tumor microenvironment promotes cancer growth through multiple mechanisms (26). In CML, imatinib resistance shifts BCR-ABL1$^+$ cells to a glycolytic phenotype with elevated glucose uptake and lactate production (27), and this phenotype protects cells from apoptosis (28).

Here, we assess the effect of Tri-CAP treatment on expression of glucose transporters and glycolytic enzymes at the RNA and protein levels using qRT-PCR and Western blot analysis, respectively. We note that, in response to 60-s Tri-CAP treatment, messenger RNA (mRNA) levels of *Glut1*, *Hk2*, and *Pdk1* in BCR-ABL1^{T315I} cells increase at 6-h posttreatment and then decrease over time, showing a minimum at 48-h posttreatment (final time point measured), whereas levels of *Pdk3* and *Ldha* mRNA decrease steadily over time (*SI Appendix*, Fig. S9). Similar expression patterns are observed in BCR-ABL1^{p210} cells, although parental cells show a minimal decrease in *Hk2* and *Ldha* and increased expression of *Glut1*, *Pdk1*, and *Pdk3*. Likewise, in therapy-resistant BCR-ABL1^{T315I} cells, protein expression levels of PKM2, pyruvate kinase M1/2, HK1, HK2, and PDK1 decrease progressively from 0- to 48-h post–Tri-CAP treatment, including a near complete loss of HK1 (Fig. 3*E*). At 48 h, expression levels of these proteins are reduced, albeit less so, in BCR-ABL1^{p210} cells, and their levels are fully recovered from an initial drop in parental cells. Consistent with the reduced mRNA levels of *Ldha* observed at 48 h in both BCR-ABL1$^+$ lines, lactate production in these cells is reduced by 40 to 63% at 48 h (*SI Appendix*, Fig. S10 and Table S5). Together, these data suggest that Tri-CAP blocks glycolysis at multiple major enzymatic points and significantly reduces

lactate production in resistant BCR-ABL1^{T315I} cells, with minimal and reversible impacts on parental cells.

Tri-CAP Attenuates Oncogenic Proliferative Signaling in Cancer Cells. The blockade of multiple glycolytic enzymes attenuates cross-talk with other cancer survival pathways, thereby preventing reciprocal activation. For example, PKM2 inhibition reduces glucose flux to the PPP and NADPH production. In turn, this limits NADPH-mediated synthesis of macromolecules for cancer growth (29) and attenuates NADPH-mediated renewal of GSH to disrupt redox balance (Fig. 3*F*). Similarly, LHDA is involved in cancer progression (30), and its inhibition compromises cancer stem and progenitor cells (31), whereas lactate amplifies phosphoinositide 3-kinase (PI3K)/AKT signaling (32). This suggests that Tri-CAP–induced inhibition of lactate production and LHDA expression can block glycolytic activation of PI3K/AKT signaling.

The PI3K/AKT/mammalian target of rapamycin (mTOR) pathway is one of the most commonly activated signaling pathways in human cancers, with its activation leading to therapy resistance (33). AKT stimulates glycolysis by promoting ATP generation and inducing the expression of glycolytic enzymes, whereas mTOR activates transcription factors, such as HIF-1α, that promote the expression of glycolytic enzymes involved in cancer progression (34). Conversely, lactate production from glycolysis amplifies PI3K/AKT signaling (32). Such reciprocal activation between glycolysis and PI3K/AKT/mTOR/HIF-1α signaling perpetuates cancer survival (32–34) (*SI Appendix*, Fig. S11). In CML, it has further been shown that BCR-ABL1 signaling elevates HIF-1α activity, and HIF-1α overexpression promotes imatinib resistance (35), suggesting that HIF-1α inhibition is likely to improve therapeutic outcome. We therefore evacuate the effect of Tri-CAP on HIF-1α and AKT/mTOR signaling in CML cell lines.

At 6-h posttreatment, protein expression of HIF-1α is reduced to 30 and 34% in BCR-ABL1^{T315I} and BCR-ABL1^{p210} cells, respectively, whereas the expression in parental cells is mostly unaffected (Fig. 3*G*). Similarly, at 6 h, the expression of phosphorylated mTOR at serine (S)2448 is reduced significantly in BCR-ABL1^{T315I} (to 36%), less so in BCR-ABL1^{p210} cells (to 46%), and the least in the parental cells (to 83%). Expression of phosphorylated AKT at threonine (T)308 decreases to 69% in BCR-ABL1^{T315I} but increases by 11 to 13% in BCR-ABL1^{p210} and parental cells (Fig. 3*G*). Phosphorylated AKT at S473 is less informative since it is poorly correlated to AKT protein activity (36, 37). These data indicate that Tri-CAP preferentially disrupts AKT/mTOR/HIF-1α signaling in imatinib-resistant BCR-ABL1^{T315I} cells, as compared to parental cells and BCR-ABL1^{p210} cells (Fig. 3*H*). Interestingly, this preferential disruption strengthens after 6 h with the protein expression of HIF-1α falling to a negligible level in BCR-ABL1^{T315I} cells at 24 to 48 h but rising from 24 to 48 h in parental and BCR-ABL1^{p210} cells (*SI Appendix*, Fig. S12). Taken together, results from these experiments and the preceding two sections demonstrate that Tri-CAP preferentially blocks the three key cancer survival pathways—redox deregulation, glycolysis, and proliferative AKT/mTOR/HIF-1α signaling—in resistant BCR-ABL1^{T315I}, thus uncovering a previously uncharted paradigm for cancer treatment and resistance abatement.

It is unknown whether a single therapy could induce a simultaneous blockade of the three cancer cell survival pathways, particularly with ROS-generating strategies that often inadvertently promote cancer cell survival with therapy-produced ROS (19). This risk is also noted with current CAP systems that are shown to up-regulate cellular antioxidant systems (38) and produce H_2O_2 above its threshold for activation of the oncogenic HIF-1a signaling (*SI Appendix*, Fig. S1). Our finding suggests a previously unknown avenue to overcoming cancer cell survival and, hence, therapy resistance.

Tri-CAP Selectively Induces Apoptosis in Therapy-Resistant Cancer Cell Lines. To further explore the mechanism by which Tri-CAP induces lethality in therapy-resistant cells, we again use the mouse Ba/F3 cell line model of CML. Notably, we find that 60-s Tri-CAP treatment reduces viability of BCR-ABL1^{T315I} and BCR-ABL1^{p210} cells to ∼2 and ∼3%, respectively, at 24- and 72-h posttreatment, with negligible effects on parental cells at 72 h (Fig. 4*A*). Pretreatment with *N*-acetyl-L-cysteine, an ROS scavenger, largely rescues both BCR-ABL1^{+} lines, while minimally affecting parental cells (*SI Appendix*, Fig. S13), indicating that Tri-CAP acts largely through ROS. Tri-CAP reduction of BCR-ABL1^{+} cells to 2 to 3% viability with exceptional selectivity highlights a distinct mode of action. This is in contrast of 15 to 40% viability seen with current CAP jets (39) that are only modestly selective. Analysis of apoptosis at 24-h post–Tri-CAP treatment further reveals apoptotic cell levels of 75, 44, and 37% in BCR-ABL1^{T315I}, BCR-ABL1^{P210}, and parental cells, respectively (Fig. 4 *B* and *C*), revealing preferentially increased vulnerability of resistant cells. Notably, the 75% apoptosis rate in T315I-mutant cells in response to Tri-CAP is much higher than that observed with imatinib (25 to 40%) (40) and current, redox-targeting drugs (40 to 50%), such as arsenic trioxide (41), which suggests that it utilizes a distinct mode of action.

We find that Tri-CAP–induced death of BCR-ABL1^{T315I} cells is significantly reduced by pan-caspase inhibitor and modestly reduced by necrosis inhibitor (*SI Appendix*, Fig. S14 *A–C*). Furthermore, Tri-CAP appears to induce ferroptosis by elevating cellular irons, increasing expression of ferroptosis-promoting nuclear receptor coactivator 4 and reducing protein expression of glutathione peroxidase 4 and Kelch-like ECH-associated protein 1 that suppress ferroptosis (*SI Appendix*, Fig. S14 *D* and *E*). Given significant apoptosis rate (Fig. 4*C*) and that glycolysis and HIF-1α pathways, both potently disrupted by Tri-CAP, are intimately associated with apoptosis (42, 43), Tri-CAP lethality in resistant BCR-ABL1^{T315I} cells appears to be predominately through apoptosis, with ferroptosis and necrosis also playing a role.

AR230^{R}, A375, and BT-474 are therapy-resistant human CML, melanoma, and breast cancer cell lines, respectively, with mutations in different oncogenic kinases of BCR-ABL1, BRAF, and HER2, respectively. Their resistance mechanisms are varied, including those independent of kinase mutation, for example, Ras/Mek/Erk or PI3K/AKT signaling (44, 45). Despite these significant differences in resistance mechanisms, viability of these cells is similarly reduced by Tri-CAP to 2.8 to 7.5% of control (*SI Appendix*, Fig. S15). Tri-CAP treatment for more than 60 s adds a limited benefit of 0 to 3% further reduction in cell viability. Collectively, these data demonstrate potent anticancer activity of Tri-CAP in diverse malignant cells, including the mouse Ba/F3 cell line model of therapy-resistant CML and three therapy-resistant human cancer cell lines associated with disparate resistance mechanisms.

Tri-CAP Induces High-Rate Apoptotic Death in CD34^{+} Hematopoietic Stem and Progenitor Cells from CML Patients. CD34^{+} cells, including hematopoietic stem and progenitor cells, are difficult to eliminate in CML, even with treatments such as imatinib that can normalize blood counts. Here, we find that 60-s Tri-CAP treatment reduces viability of CD34^{+} hematopoietic stem and progenitor cells from CML patients with the T315I mutation to 11.98 ± 2.21% ($P < 0.001$) of the untreated controls at 72 h, whereas cells from healthy individuals are only reduced to 82.83 ± 9.65% ($P < 0.001$), suggesting selective lethality in CML patient cells with the T315I mutation (*SI Appendix*,

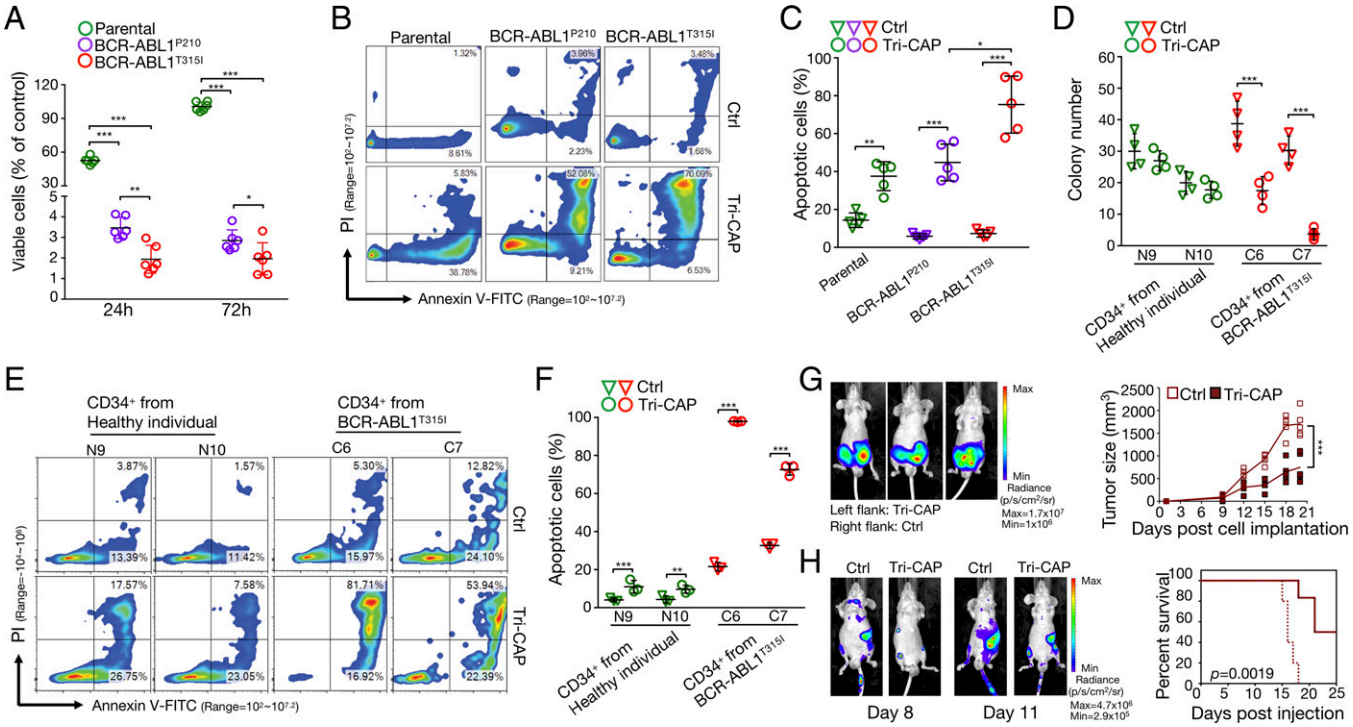

Fig. 4. Tri-CAP induces selective apoptotic death of resistant BCR-ABL1^{T315I} cells. (*A*) Viability of BCR-ABL1^{+} and parental cells at 24- and 72-h post–Tri-CAP treatment for 60 s (n = 6). Flow cytometry analysis of apoptosis (*B*) and percent apoptotic cells at 24-h post–Tri-CAP treatment in BCR-ABL1^{+} and parental cells (n = 5) (*C*). (*D*) Number of colonies formed 7 to 14 d following Tri-CAP treatment with primary CD34^{+} hematopoietic stem and progenitor cells from CML patients with T315I (C6 and C7) and cells from healthy individuals (N9 and N10); cells are described in *SI Appendix*, Table S6 (n = 4). Flow cytometry analysis of apoptosis (*E*) and percent apoptotic cells at 24-h post–Tri-CAP treatment for primary CD34^{+} hematopoietic stem and progenitor cells from CML patients with T315I and healthy controls (n = 3) (*F*). (*G*) Mouse tumor model of CML: Left panel shows bioluminescence images of tumors on day 20 in engrafted nude mice that were subcutaneously injected with BCR-ABL1^{T315I} cells, with (left flank) or without (right flank) Tri-CAP treatment; graph of tumor size over time is shown at right (n = 5). (*H*) In the mouse survival model of CML, Tri-CAP–treated or untreated (Ctrl) BCR-ABL1^{T315I} cells were injected into the tail veins of nude mice; left panel shows bioluminescence images of nude mice engrafted with Ctrl and Tri-CAP–treated BCR-ABL1^{T315I} cells on days 8 and 11, and right panel shows percent survival of engrafted mice over time (n = 5). *P < 0.05, **P < 0.01, and ***P < 0.001.

Fig. S16). Next, we assess colonies of Tri-CAP–treated CD34^{+} hematopoietic stem and progenitor cells and observe reduced colony formation relative to control-treated cells for the two BCR-ABL1^{T315I} patient samples (17.50 ± 4.43%, P < 0.01; 3.75 ± 1.71%, P < 0.001) and for two samples from patients with native BCR-ABL1 (18.25 ± 3.59%, P < 0.01; 0.50 ± 0.58%, P < 0.001) (Fig. 4*D* and *SI Appendix*, Figs. S17 and S18). In contrast, there is no statistically significant difference between untreated and Tri-CAP–treated CD34^{+} cells from healthy individuals. Furthermore, we detect increased apoptosis rates relative to control in Tri-CAP–treated CD34^{+} cells from two patients with BCR-ABL1^{T315I}; rates increased to 98.36 ± 0.24% (P < 0.001) and 75.01 ± 1.08% (P < 0.01) from 19.76 ± 2.07% and 32.60 ± 2.86%, respectively (Fig. 4 *E* and *F*). These values contrast sharply with the low-apoptosis rates of 16.81 to 30.14% observed in CD34^{+} cells from healthy individuals. As cancer stem and progenitor cells are resistant to most therapies, including ROS-targeting radiotherapy (46), the very high apoptosis rate of 75.01 to 98.36% in Tri-CAP–treated CD34^{+} CML patient cells is noteworthy and may result from Tri-CAP–mediated inhibition of LHDA, which is known to lead to the killing of cancer stem and progenitor cells (30).

Tri-CAP Attenuates Tumor Growth and Improves Survival of Tumor-Bearing Mice. Therapeutics for CML are commonly tested using a mouse tumor model and a mouse survival model of this disease (47). Here, using the tumor model, we subcutaneously inject equal numbers of Tri-CAP–treated and untreated mouse BCR-ABL1^{T315I} cells into the left and right flanks of each nude mouse, respectively. We find that Tri-CAP–treated T315I-mutant cells generate tumors that display reduced growth relative to those from untreated cells (Fig. 4*G*). At day 20 post-injection, mean tumor volume of treated BCR-ABL1^{T315I} cells is measured at 747.6 ± 275.2 mm^3, corresponding to a reduction of 56.2% from the mean volume of 1,705.6 ± 254.7 mm^3 detected in untreated cells (P < 0.001). Similarly, tumors derived from treated BCR-ABL1^{p210} cells are smaller than those from untreated cells (*SI Appendix*, Fig. S19). In the mouse survival model, we intravenously inject equal numbers of untreated or Tri-CAP–treated mouse BCR-ABL1^{T315I} cells into the tail veins of nude mice. All mice injected with untreated BCR-ABL1^{T315I} cells die by day 18 (Fig. 4*H*). In contrast, mice injected with treated BCR-ABL1^{T315I} cells display survival rates of 50% on day 25. Similarly, all mice bearing untreated BCR-ABL1^{p210} cells die on day 18, whereas the survival rate of mice bearing treated BCR-ABL1^{p210} cells is 67% on day 25 (*SI Appendix*, Fig. S20). These data demonstrate that Tri-CAP treatment reduces tumor formation and improves the survival of tumor-bearing mice.

To test against an established tumor, we subcutaneously implant luciferase-carrying BCR-ABL1^{T315I} cells into the rear dorsum of mice, allow for the tumor to form for 6 d, and treat them with 120 s Tri-CAP once every 3 d (*SI Appendix*, Fig. S21*A*). Tumors in the Tri-CAP group are smaller than the control group; the mean volume of treated tumors at 871.3 ± 52.07 cm^3 on day 18 is 48% of 1,807 ± 14.49 cm^3 in untreated mice (P < 0.0001) (*SI Appendix*, Fig. S21 *B–D*). Also, Tri-CAP prolongs the survival of tumor-bearing mice (*SI Appendix*,

Fig. S21*E*). Next, we prepare PAS in saline pretreated with 120 s Tri-CAP and inject it to pericarcinomatous tissues once every 3 d (*SI Appendix*, Fig. S22*A*). Treated tumors are significantly reduced (*SI Appendix*, Fig. S22 *B–D*): The tumor volume on day 18 is 849.9 ± 40.03 cm^3 in the PAS group, 49.2% smaller than 1,725 ± 88.51 cm^3 in the saline group ($P < 0.0001$; *SI Appendix*, Fig. S22*D*). Furthermore, PAS prolongs the survival of tumor-bearing mice (*SI Appendix*, Fig. S22*E*).

For many hematological malignancies, stem cell transplantation is the only therapeutic option; however, it is limited by relapse and poor prognosis, for example, a 2-y survival rate of <20% for acute myeloid leukemia (48). This procedure involves apheresis, to which Tri-CAP may be incorporated for extracorporeal treatment of patient blood. This option is supported by the selective potency of Tri-CAP in $CD34^+$ stem and progenitor cells from CML patients (Fig. 4 *D–F* and *SI Appendix*, Figs. S16–S18). Notably, PAS is approved for treatment of human patients in clinical trials (15) and may be administrated as an intraperitoneal (16) or infusion therapy, for example, to bone marrow that is metastasized by solid tumors (49). Our in vivo study in *SI Appendix*, Fig. S22 shows that PAS prepared with Tri-CAP is readily amendable for intraperitoneal or infusion administration. These examples illustrate just a few potential administration options for Tri-CAP.

Conclusion

Cancer cells are exceptionally flexible in their ability to leverage metabolic conditions, signaling molecules, stromal elements, and other factors for their survival. Furthermore, they exploit reciprocal activation between survival pathways, such as PI3K/AKT activation of glycolytic enzymes (34) and glycolytic amplification of PI3K/AKT signaling through LHDA expression and/or lactate production (30–32). Collectively, these present a considerable roadblock to strategies aimed at targeting only a limited number of molecules, as evident from clinical data on current inhibitors that target glycolysis (8), proliferative signaling (34), or redox deregulation (9). An ideal strategy to combat therapy resistance would induce a system-level blockade of many cancer survival pathways, as well as their reciprocal activation, with little toxicity. Our study is a first attempt toward this goal with Tri-CAP. Using a mouse cell line model of therapy-resistant CML, we show that Tri-CAP preferentially induces a multitargeted blockade of three major cancer survival pathways of deregulated redox balance, glycolysis, and AKT/mTOR/HIF-1α signaling in resistant BCR-$ABL1^{T315I}$ cells. This system-level disruption leads to substantial lethality in cell lines and $CD34^+$ hematopoietic stem and progenitor cells from CML patients harboring the therapy-resistant BCR-$ABL1^{T315I}$ mutation, as well as other therapy-resistant breast cancer, melanoma, and CML cell lines with diverse resistance mechanisms, while having minimal impact on nonmalignant cells. In addition, Tri-CAP attenuates tumor formation, reduces established tumor, and improves the survival of tumor-bearing mice. Distinctly, Tri-CAP induces exceptionally high rates of apoptosis (i.e., 75 to 98%) in resistant BCR-$ABL1^{T315I}$ cell lines and $CD34^+$ hematopoietic stem and progenitor cells from CML patients, which are far above the rates of 25 to 40% observed with the current standard of care targeted therapies for CML patients (40) and the rates of 40 to 50% achieved with redox-targeting therapies (41). This likely results from Tri-CAP–mediated blockade of multiple cancer survival pathways and their reciprocal activation.

Cancer therapies based on ROS-generating strategies, including radiotherapy, are not new and usually rely on high levels of ROS to induce direct cancer cell death (9, 50). Ironically, the brute force strategy of cytotoxic ROS promotes stress responses that favor cell survival. For example, iodine-125 seeds radiation therapy damages cancer cell DNA, but its damaged mitochondria releases ROS to promote oncogenic HIF-1α (19). Given this, we aim instead to starve cancer cells to death by blocking many of their survival pathways that are similarly susceptible to regulation and, hence, disruption with ROS. Significantly, this common vulnerability of multiple cancer survival pathways is potently exploited by Tri-CAP, which produces exceptionally low-level, transient, and diverse ROS, resulting in selective induction of high-rate apoptosis in therapy-resistant cell lines and primary $CD34^+$ hematopoietic stem and progenitor cells from CML patients. As deregulated redox balance, glycolysis, and AKT/mTOR/HIF-1α signaling are among the most commonly activated survival pathways in human cancers (7, 34), their system-level blockade by Tri-CAP suggests a broadly applicable strategy for resistance abatement. Importantly, PAS prepared with Tri-CAP demonstrates similar efficacy to Tri-CAP in reducing the established tumor and promoting the survival of tumor-bearing animals (*SI Appendix*, Figs. S21 and S22) and is therefore expected to be similarly potent in blocking multiple cancer survival pathways. Further investigations exploring the clinical utility of these strategies are therefore warranted. Tri-CAP and PAS may be used in combination with existing therapies (13) or as a monotherapy (14), with multiple administration options, including as infusion, transdermal, and extracorporeal therapies. Collectively, our results provide a basis for future clinical studies and demonstrate the potential utility of Tri-CAP as a potent strategy for overcoming and preventing therapy resistance in a variety of malignancies.

Materials and Methods

Primary Human Cells. Mononuclear cells from the peripheral blood of patients with chronic-phase CML or from cord blood of healthy individuals were separated by Ficoll gradient, and the $CD34^+$ fraction was isolated using an autoMACS Pro (Miltenyi Biotech) at Huntsman Cancer Institute, University of Utah. Purity was determined to be >90% by flow cytometry (51). Prior to use in assays, $CD34^+$ cells from CML patients were cultured overnight in RPMI-1640 medium, containing 20% BIT9500 (Stem Cell Technologies), 100 U/mL penicillin–streptomycin, and 2 mM L-glutamine (Gibco Life Technologies), without the addition of cytokines. Where indicated, 96-h $CD34^+$ CML cell assays were performed in the absence of cytokines. BCR-ABL1 sequence was confirmed in all cells using conventional bidirectional Sanger sequencing with BigDye terminator chemistry on an ABI3730 instrument. All patients provided their informed consent in accordance with the Declaration of Helsinki, and all studies with human specimens were approved by the University of Utah Institutional Review Board (Protocol #45880). Primary cells are described in *SI Appendix*, Table S6.

Tri-CAP Generation and Cell Treatment. Tri-CAP was generated using a plasma jet with argon (99.9% purity) mixed with 3% oxygen (99.9% purity) as a carrier gas, flowing at 1.9 L/min. The high-voltage electrode is a stainless-steel rod, with a 1.61-mm diameter and is housed in a concentric quartz tube, with an inner diameter of 3.91 mm and an outer diameter of 6.34 mm. A 20-mm-wide copper foil is wrapped around the quartz tube as the grounded electrode. Its edge on the side of the tube nozzle is leveled to the tip of the rod electrode, and both are 30 mm from the surface of the cell medium in a Petri dish (*SI Appendix*, Fig. S1*A*). The tube nozzle is 20 mm from the cell medium surface. Temperature and pH of cell-free media are measured with a thermal couple and a pH meter. Cells seeded at a suitable concentration in 12-well plates are treated with Tri-CAP at room temperature; treatment time was 60 s, except for human cell lines, which are treated for 60 to 150 s. After treatment, the cells are incubated without medium change at 37 °C before assaying. Control gas-only samples are treated with the $Ar+O_2$ gas, flowing at 1.9 L/min, for the same duration as the Tri-CAP treatment group in a biosafety cabinet at room temperature.

Detailed materials and methods are provided in *SI Appendix*, where the reader may also find a broad set of additional results and analysis.

Data Availability. All data presented in this study are included in the article and/or *SI Appendix*.

ACKNOWLEDGMENTS. This work is supported by a Frank Batten Chair Endowment at Old Dominion University. H.-L.C. and M.G.K. thank Dr. Brian

Druker of Oregon Health and Science University for the generous gift of Ba/F3 cell lines and for his advice. B.G., W.L., M.Q., and C.H. acknowledge the support of the National Natural Science Foundation of China (Grant 51837008). A.D.P. and M.W.D. thank Kimberly R. Reynolds and Phillip M. Clair of the Huntsman Cancer Institute at the University of Utah for patient sample processing and inventory management.

1. C. Holohan, S. van Schaeybroeck, D. B. Longley, P. G. Johnston, Cancer drug resistance: An evolving paradigm. *Nat. Rev. Cancer* **13**, 714–726 (2013).
2. J. Rueff, A. S. Rodrigues, Cancer drug resistance: A brief overview from a genetic viewpoint. *Methods Mol. Biol.* **1395**, 1–18 (2016).
3. S. Batson *et al.*, Tyrosine kinase inhibitor combination therapy in first-line treatment of non-small-cell lung cancer: Systematic review and network meta-analysis. *Onco. Targets Ther.* **10**, 2473–2482 (2017).
4. J. S. Khorashad *et al.*, BCR-ABL1 compound mutations in tyrosine kinase inhibitor-resistant CML: Frequency and clonal relationships. *Blood* **121**, 489–498 (2013).
5. M. Maemondo *et al.*, North-East Japan Study Group, Gefitinib or chemotherapy for non-small-cell lung cancer with mutated EGFR. *N. Engl. J. Med.* **362**, 2380–2388 (2010).
6. G. V. Long *et al.*, Increased MAPK reactivation in early resistance to dabrafenib/trametinib combination therapy of BRAF-mutant metastatic melanoma. *Nat. Commun.* **5**, 5694 (2014).
7. D. Hanahan, R. A. Weinberg, Hallmarks of cancer: The next generation. *Cell* **144**, 646–674 (2011).
8. R. A. Cairns, I. S. Harris, T. W. Mak, Regulation of cancer cell metabolism. *Nat. Rev. Cancer* **11**, 85–95 (2011).
9. D. Trachootham, J. Alexandre, P. Huang, Targeting cancer cells by ROS-mediated mechanisms: A radical therapeutic approach? *Nat. Rev. Drug Discov.* **8**, 579–591 (2009).
10. M. D. Jacobson, Reactive oxygen species and programmed cell death. *Trends Biochem. Sci.* **21**, 83–86 (1996).
11. A. Silva *et al.*, Intracellular reactive oxygen species are essential for PI3K/Akt/mTOR-dependent IL-7-mediated viability of T-cell acute lymphoblastic leukemia cells. *Leukemia* **25**, 960–967 (2011).
12. M. G. Kong *et al.*, Plasma medicine: An introductory review. *New J. Phys.* **11**, 110512 (2009).
13. M. E. Ruidiaz *et al.*, Quantitative comparison of surgical margin histology following excision with traditional electrosurgery and a low-thermal-injury dissection device. *J. Surg. Oncol.* **104**, 746–754 (2011).
14. H.-R. Metelmann *et al.*, Clinical experience with cold plasma in the treatment of locally advanced head and neck cancer. *Clin. Plasma Med.* **9**, 6–13 (2018).
15. S. Zhai *et al.*, Successful treatment of vitiligo with cold atmospheric plasma-activated hydrogel. *J. Invest. Dermatol.* **141**, 2710–2719.e6 (2021).
16. S. Takeda *et al.*, Intraperitoneal administration of plasma-activated medium: Proposal of a novel treatment option for peritoneal metastasis from gastric cancer. *Ann. Surg. Oncol.* **24**, 1188–1194 (2017).
17. G. Chen *et al.*, Transdermal cold atmospheric plasma-mediated immune checkpoint blockade therapy. *Proc. Natl. Acad. Sci. U.S.A.* **117**, 3687–3692 (2020).
18. W. Tian, M. J. Kushner, Atmospheric pressure dielectric barrier discharges interacting with liquid covered tissue. *J. Phys. D Appl. Phys.* **47**, 165201 (2014).
19. L. Hu, H. Wang, L. Huang, Y. Zhao, J. Wang, The protective roles of ROS-mediated mitophagy on ^{125}I seeds radiation induced cell death in HCT116 cells. *Oxid. Med. Cell. Longev.* **2016**, 9460462 (2016).
20. E. Jabbour *et al.*, Combination of hyper-CVAD with ponatinib as first-line therapy for patients with Philadelphia chromosome-positive acute lymphoblastic leukaemia: Long-term follow-up of a single-centre, phase 2 study. *Lancet Haematol.* **5**, e618–e627 (2018).
21. N. S. Chandel *et al.*, Reactive oxygen species generated at mitochondrial complex III stabilize hypoxia-inducible factor-1alpha during hypoxia: A mechanism of O_2 sensing. *J. Biol. Chem.* **275**, 25130–25138 (2000).
22. X. Yan *et al.*, Plasma-induced death of HepG2 cancer cells: Intracellular effects of reactive species. *Plasma Process. Polym.* **9**, 59–66 (2012).
23. C. Chen, F. Li, H.-L. Chen, M. G. Kong, Aqueous reactive species induced by a PCB surface micro-discharge air plasma device: A quantitative study. *J. Phys. D Appl. Phys.* **50**, 445208 (2017).
24. Y. Gorbanev, D. O'Connell, V. Chechik, Non-thermal plasma in contact with water: The origin of species. *Chemistry* **22**, 3496–3505 (2016).
25. M. Warmuth, S. Kim, X.-j. Gu, G. Xia, F. Adrián, Ba/F3 cells and their use in kinase drug discovery. *Curr. Opin. Oncol.* **19**, 55–60 (2007).
26. M. Apicella *et al.*, Increased lactate secretion by cancer cells sustains non-cell-autonomous adaptive resistance to MET and EGFR targeted therapies. *Cell Metab.* **28**, 848–865.e6 (2018).
27. D. J. Kominsky *et al.*, Abnormalities in glucose uptake and metabolism in imatinib-resistant human BCR-ABL-positive cells. *Clin. Cancer Res.* **15**, 3442–3450 (2009).
28. E. F. Mason *et al.*, Aerobic glycolysis suppresses p53 activity to provide selective protection from apoptosis upon loss of growth signals or inhibition of BCR-Abl. *Cancer Res.* **70**, 8066–8076 (2010).
29. H.-Q. Ju, J.-F. Lin, T. Tian, D. Xie, R.-H. Xu, NADPH homeostasis in cancer: Functions, mechanisms and therapeutic implications. *Signal Transduct. Target. Ther.* **5**, 231 (2020).
30. A. Le *et al.*, Inhibition of lactate dehydrogenase A induces oxidative stress and inhibits tumor progression. *Proc. Natl. Acad. Sci. U.S.A.* **107**, 2037–2042 (2010).
31. H. Xie *et al.*, Targeting lactate dehydrogenase—A inhibits tumorigenesis and tumor progression in mouse models of lung cancer and impacts tumor-initiating cells. *Cell Metab.* **19**, 795–809 (2014).
32. K. Xu *et al.*, Glycolysis fuels phosphoinositide 3-kinase signaling to bolster T cell immunity. *Science* **371**, 405–410 (2021).
33. P. Liu, H. Cheng, T. M. Roberts, J. J. Zhao, Targeting the phosphoinositide 3-kinase pathway in cancer. *Nat. Rev. Drug Discov.* **8**, 627–644 (2009).
34. G. L. Semenza, Hypoxia-inducible factors: Mediators of cancer progression and targets for cancer therapy. *Trends Pharmacol. Sci.* **33**, 207–214 (2012).
35. F. Zhao *et al.*, Imatinib resistance associated with BCR-ABL upregulation is dependent on HIF-1alpha-induced metabolic reprograming. *Oncogene* **29**, 2962–2972 (2010).
36. E. E. Vincent *et al.*, Akt phosphorylation on Thr308 but not on Ser473 correlates with Akt protein kinase activity in human non-small cell lung cancer. *Br. J. Cancer* **104**, 1755–1761 (2011).
37. N. Balasuriya *et al.*, Genetic code expansion and live cell imaging reveal that Thr-308 phosphorylation is irreplaceable and sufficient for Akt1 activity. *J. Biol. Chem.* **293**, 10744–10756 (2018).
38. S. Bekeschus *et al.*, xCT (SLC7A11) expression confers intrinsic resistance to physical plasma treatment in tumor cells. *Redox Biol.* **30**, 101423 (2020).
39. E. Biscop *et al.*, The influence of cell type and culture medium on determining cancer selectivity of cold atmospheric plasma treatment. *Cancers (Basel)* **11**, 1287 (2019).
40. S. Okabe *et al.*, Efficacy of the dual PI3K and mTOR inhibitor NVP-BEZ235 in combination with nilotinib against BCR-ABL-positive leukemia cells involves the ABL kinase domain mutation. *Cancer Biol. Ther.* **15**, 207–215 (2014).
41. G.-Q. Chen *et al.*, In vitro studies on cellular and molecular mechanisms of arsenic trioxide (As_2O_3) in the treatment of acute promyelocytic leukemia: As_2O_3 induces NB4 cell apoptosis with downregulation of Bcl-2 expression and modulation of PML-RAR alpha/PML proteins. *Blood* **88**, 1052–1061 (1996).
42. N. N. Danial *et al.*, BAD and glucokinase reside in a mitochondrial complex that integrates glycolysis and apoptosis. *Nature* **424**, 952–956 (2003).
43. G. L. Semenza, Targeting HIF-1 for cancer therapy. *Nat. Rev. Cancer* **3**, 721–732 (2003).
44. P. I. Poulikakos, N. Rosen, Mutant BRAF melanomas—Dependence and resistance. *Cancer Cell* **19**, 11–15 (2011).
45. R. Nahta, D. Yu, M.-C. Hung, G. N. Hortobagyi, F. J. Esteva, Mechanisms of disease: Understanding resistance to HER2-targeted therapy in human breast cancer. *Nat. Clin. Pract. Oncol.* **3**, 269–280 (2006).
46. M. Diehn *et al.*, Association of reactive oxygen species levels and radioresistance in cancer stem cells. *Nature* **458**, 780–783 (2009).
47. T. O'Hare *et al.*, AP24534, a pan-BCR-ABL inhibitor for chronic myeloid leukemia, potently inhibits the T315I mutant and overcomes mutation-based resistance. *Cancer Cell* **16**, 401–412 (2009).
48. P. Tsirigotis *et al.*, Relapse of AML after hematopoietic stem cell transplantation: Methods of monitoring and preventive strategies. A review from the ALWP of the EBMT. *Bone Marrow Transplant.* **51**, 1431–1438 (2016).
49. R. Coleman, M. Gnant, G. Morgan, P. Clezardin, Effects of bone-targeted agents on cancer progression and mortality. *J. Natl. Cancer Inst.* **104**, 1059–1067 (2012).
50. H. Sies, D. P. Jones, Reactive oxygen species (ROS) as pleiotropic physiological signalling agents. *Nat. Rev. Mol. Cell Biol.* **21**, 363–383 (2020).
51. A. D. Pomicter *et al.*, Femoral heads from total hip arthroplasty as a source of adult hematopoietic cells. *Acta Haematol.* **144**, 458–464 (2021).